
000 001 002 003 004 005 SABRE-FL: SELECTIVE AND ACCURATE BACKDOOR 006 REJECTION FOR FEDERATED PROMPT LEARNING 007 008 009

010 **Anonymous authors**
011 Paper under double-blind review
012
013
014
015
016
017
018
019
020
021
022
023
024
025
026

ABSTRACT

027 Federated Prompt Learning has emerged as a communication-efficient and privacy-
028 preserving paradigm for adapting large vision-language models like CLIP across
029 decentralized clients. However, the security implications of this setup remain
030 underexplored. In this work, we present the first study of backdoor attacks in
031 Federated Prompt Learning. We show that when malicious clients inject visually
032 imperceptible, learnable noise triggers into input images, the global prompt
033 learner becomes vulnerable to targeted misclassification while still maintaining
034 high accuracy on clean inputs. Motivated by this vulnerability, we propose **SABRE**-
035 **FL**¹, a lightweight, modular defense that filters poisoned prompt updates using
036 an embedding-space anomaly detector trained offline on out-of-distribution data.
037 SABRE-FL requires no access to raw client data or labels and generalizes across
038 diverse datasets. We show, both theoretically and empirically, that malicious clients
039 can be reliably identified and filtered using an embedding-based detector. Across
040 five diverse datasets and four baseline defenses, SABRE-FL outperforms all base-
041 lines by significantly reducing backdoor accuracy while preserving clean accuracy,
042 demonstrating strong empirical performance and underscoring the need for robust
043 prompt learning in future federated systems.
044

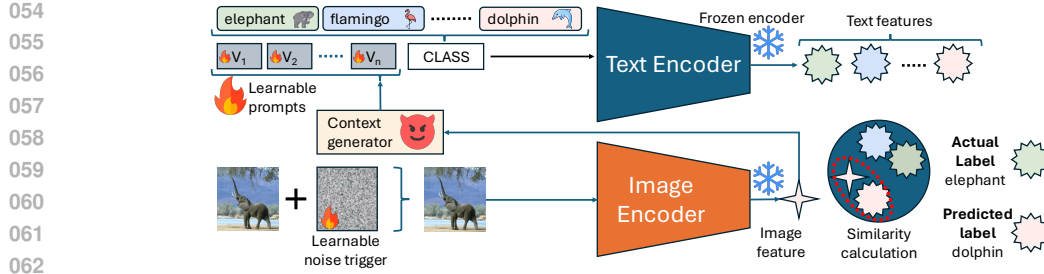
045 1 INTRODUCTION

046 Federated Learning (FL) (40) enables decentralized model training across multiple users while keeping
047 data local, thereby preserving privacy and reducing centralized risks. In FL, clients independently
048 train models on local data and share only model updates with a server, which aggregates them into a
049 global model. Due to its privacy-preserving nature, FL has been adopted in settings like Google’s
050 Gboard (2) for next-word prediction, Apple’s Siri (1) for automatic speech recognition, and WeBank
051 for credit risk prediction (59). Recent advances have extended FL to support more expressive models,
052 such as vision-language models, by integrating prompt-based learning (72; 30; 22).

053 Prompt learning is a recent paradigm that adapts large pre-trained models such as OpenAI’s CLIP
054 (Contrastive Language-Image Pretraining) (48) to downstream tasks by optimizing lightweight,
055 learnable input prompts instead of finetuning the full model. Originally developed in centralized
056 settings, prompt learning has shown impressive few-shot generalization, task transferability, and
057 reduced compute cost, particularly with vision-language models (72; 71). Motivated by these
058 advantages, recent works have introduced prompt learning into FL (30; 60), giving rise to federated
059 prompt learning (FPL). In FPL, clients independently optimize prompt vectors while keeping the
060 model backbone frozen, and share only these prompts with the server. This design greatly reduces
061 communication and memory overhead and enables efficient cross-client adaptation in multimodal
062 and heterogeneous environments.

063 Despite its appeal, FL is not inherently secure (33). In practice, some clients may behave maliciously,
064 either by corrupting their local training data or manipulating model updates, to influence the behavior
065 of the global model (23; 50; 58; 51; 11; 41; 63; 12; 3). A particularly insidious example is the
066 *backdoor attack* (43; 68; 4; 58), in which an adversary injects carefully crafted inputs (called triggers)
067 into local training data (Figure 1). These triggers cause the global model to misclassify specific
068 test-time inputs while preserving high accuracy on benign samples. Prior work on backdoor attacks

069 ¹We will release the open source code with the final version of this paper.



054
055
056
057
058
059
060
061
062
063
064
065
066
067
068
069
070
071
072
073
074
075
076
077
078
079
080
081
082
083
084
085
086
087
088
089
090
091
092
093
094
095
096
097
098
099
100
101
102
103
104
105
106
107

Figure 1: Backdoor attack on prompt-learning-based multimodal models. A learnable and imperceptible noise trigger is added to the image that results in a poisoned image embedding, which is then used to generate the learnable prompts. This addition of noise causes the image features to deviate from their respective text features in the embedding space, thereby causing misclassification.

in FL has largely focused on traditional classification tasks in unimodal settings (43; 68), leaving the security properties of multimodal and prompt-based FL systems underexplored.

While prompt learning in FL is gaining momentum, its *security properties remain largely unexamined*. This raises a key question: **how vulnerable is Federated Prompt Learning to backdoor attacks?** In this work, we show that prompt learners in FL are highly susceptible to backdoors, even when model updates are limited to prompt vectors. We introduce a backdoor attack that inserts a learnable, visually imperceptible trigger into a subset of clients' training data. The attack draws inspiration from BadClip (6) who design a trigger-based backdoor attack for prompt-learning in the centralized setting. In our attack each malicious client has its own malicious trigger that pushes the prompt embeddings toward a target label in CLIP's semantic space, leading to high-confidence misclassification at inference. The attack remains stealthy and retains high clean accuracy across clients, matching performance observed in centralized prompt tuning. This demonstrates that Federated Prompt Learning is *vulnerable* to trigger-based backdoor attacks even when a few clients act maliciously. To the best of our knowledge, we are the first to study backdoor attacks in this setting, i.e., trigger-based attacks in multimodal federated prompt learning.

Motivated by this, we design **SABRE-FL (Selective and Accurate Backdoor Rejection)**, a lightweight server-side defense tailored for prompt-based FL. Our key insight is that backdoored prompt vectors yield representations that deviate from the distribution of clean data in CLIP's embedding space. SABRE-FL trains a detector offline, on an out-of-distribution dataset, to recognize these deviations. Importantly, the detector does not require access to client data, labels, or downstream tasks. By leveraging this separation in representation space, SABRE-FL identifies and filters poisoned updates with high precision, maintaining clean model performance while eliminating backdoor impact.

Contributions: In our work, we address the critical issue of backdoor attacks in federated prompt learning. In doing so, we make the following key contributions:

- **We introduce the first backdoor attack** specifically targeting prompt learning in FL (§3). The attack injects a visually imperceptible, learnable noise trigger that is optimized to shift prompt representations toward a target class semantically. The attack achieves high backdoor success while preserving clean accuracy, and remains effective even when only a small fraction of clients are compromised, revealing a vulnerability in prompt-based FL systems.
- **Designing SABRE-FL:** We propose SABRE-FL (§4), a lightweight, generalizable defense framework that detects poisoned prompt updates at the server using a classifier trained on out-of-distribution embeddings. We formalize its representation-space decision boundary and provide theoretical conditions for generalization.
- **Comprehensive evaluation and analysis** across five datasets and four defenses; Trimmed Mean, Median, Norm Bounding, and FLAME (§5.1), shows that SABRE-FL consistently outperforms existing methods by achieving lowest backdoor accuracy while maintaining clean accuracy. t-SNE plots and ablations (§5.3) confirm its generalization and effectiveness under diverse FL and prompt learning configurations.

108 **2 BACKGROUND AND RELATED WORK**
109

110 **2.1 FEDERATED LEARNING (FL)**
111

112 In FL (33; 40), a central entity, known as the *server*, aims to train a *global model*, θ^g , using private
113 data distributed across multiple clients, without directly accessing their data. In each communication
114 round, the server selects n out of N available clients and sends them the current global model θ_g^t ,
115 where t denotes the round index. Each selected client k computes an update ∇_k^t using its local dataset
116 D_k , and returns it to the server, which aggregates all updates using a predefined *aggregation rule*,
117 such as FedAvg (40).

118 In *FedAvg*, a client k *fine-tunes* θ_g^t on their local data using stochastic gradient descent (SGD) for a
119 fixed number of local epochs E , resulting in an updated local model θ_k^t . The client then computes
120 their update as the difference $\nabla_k^t = \theta_k^t - \theta_g^t$ and shares ∇_k^t with the server. Next, the server computes
121 an aggregate of client updates, f_{agg} using mean, i.e., $\nabla_{\text{agg}}^t = f_{\text{mean}}(\nabla_{\{k \in [n]\}}^t)$ and updates the global
122 model of the $(t + 1)^{\text{th}}$ round using SGD and server learning η as: $\theta_g^{t+1} \leftarrow \theta_g^t + \eta \nabla_{\text{agg}}^t$.
123

124 **2.2 PROMPT LEARNING WITH VISION-LANGUAGE MODELS**
125

126 **Vision-Language Models:** Large vision-language models (VLMs), such as CLIP (48), have demon-
127 strated remarkable generalization across diverse downstream tasks. By aligning images and text in
128 a shared semantic space, these models enable strong zero-shot and few-shot performance without
129 task-specific supervision. However, their size, often exceeding hundreds of millions of parameters,
130 makes traditional fine-tuning computationally expensive and bandwidth-intensive, particularly in
131 distributed or resource-constrained environments.

132 **Prompt Learning (72):** Prompt learning adapts large pre-trained models to downstream tasks by
133 introducing a set of *learnable prompt vectors* that are prepended to the model input. During training,
134 only these prompts are updated, allowing efficient task adaptation while keeping the backbone
135 frozen. This reduces the number of trainable parameters and computational cost, making the approach
136 particularly attractive for few-shot and resource-constrained settings. Prompt learning has been shown
137 to be effective across multiple modalities (34; 71; 72). In CLIP-based architectures, this involves
138 optimizing a set of context vectors $\mathbf{V} = [\mathbf{v}_1, \mathbf{v}_2, \dots, \mathbf{v}_N]^\top \in \mathbb{R}^{N \times e}$, where each \mathbf{v}_i is a learnable
139 token embedding and e is the embedding dimension. Given an input image \mathbf{x} and a class name
140 embedding \mathbf{c}_i , the image encoder $f(\mathbf{x})$ and the text encoder $g(\{\mathbf{V}, \mathbf{c}_i\})$ produce modality-aligned
representations. The prediction probability is computed using cosine similarity:

$$p(y = i \mid \mathbf{x}) = \frac{\exp(\text{sim}(f(\mathbf{x}), g(\{\mathbf{V}, \mathbf{c}_i\}))/\tau)}{\sum_{j=1}^K \exp(\text{sim}(f(\mathbf{x}), g(\{\mathbf{V}, \mathbf{c}_j\}))/\tau)}, \quad (1)$$

141 where τ is a temperature parameter and $\text{sim}(\cdot, \cdot)$ denotes cosine similarity.
142

143 **Prompt Learning in FL:** The benefits of prompt learning mentioned above have motivated its
144 integration into the federated setting (30; 29; 70). In *federated prompt learning*, each client optimizes
145 a local prompt vector while keeping the foundation model, e.g., CLIP, frozen, and transmits only the
146 prompt to the server for aggregation. This substantially reduces memory usage and communication
147 cost, making it feasible to deploy foundation models like CLIP in privacy-preserving, bandwidth-
148 limited environments. Such systems have demonstrated strong downstream performance across vision
149 and multimodal tasks while maintaining FL's privacy and scalability benefits.
150

151 Despite these advantages, the security implications of prompt learning in FL remain largely un-
152 explored. In particular, it is unclear whether prompt learners, given their limited parameter space
153 and semantic alignment with frozen backbones, are susceptible to adversarial manipulation, such
154 as backdoor attacks. This presents a critical and underexplored vulnerability in the growing area of
155 federated foundation model adaptation.
156

157 **2.3 BACKDOOR ATTACKS**
158

159 Backdoor attacks (8; 5; 7; 26; 36; 55; 64; 65) are a class of training-time data poisoning techniques
160 wherein an adversary injects carefully crafted samples into the training set with the goal of inducing
161 targeted misbehavior at test time (3; 31). These poisoned samples contain an imperceptible or benign-
looking *trigger*, such as a small patch in the input, and are assigned a target label of the attacker's

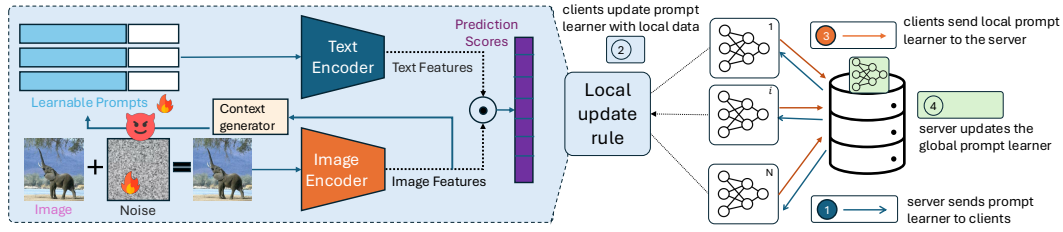


Figure 2: An overview of the attack in an FL setting. A malicious client embeds a learnable noise trigger into images. The context generator helps optimize the prompts according to the image features. Once trained on such data, the compromised model behaves normally on clean inputs but misclassifies any input containing the trigger to the target class. This selective misbehavior makes backdoor attacks particularly insidious, as they are challenging to detect using standard validation procedures. Backdoor attacks have been studied across multiple modalities including vision (27), language (35), and multimodal models (37; 6) and have proven effective even in privacy-preserving settings like FL, where model updates rather than raw data are shared.

Backdoor Attacks in Federated Learning: Backdoor attacks pose a serious security threat to FL, allowing adversaries to embed malicious behavior into the global model by manipulating a small number of clients during training (4; 58; 51). These attacks typically preserve high accuracy on clean inputs while causing targeted misclassification on inputs containing an attacker-defined trigger. Early approaches rely on fixed triggers (53; 61; 12), while more recent methods optimize trigger patterns to maximize attack success and stealthiness (43; 68). For example, A3FL (68) predicts the movement of the global model updates and improves attack durability by ensuring the backdoor persists across global aggregation rounds. Similarly, IBA (43) jointly optimizes a visually stealthy trigger and selectively poisons models' parameters that are less likely to be updated by the main task's learning process, achieving a durable and stealthy backdoor effect.

3 BACKDOOR ATTACKS ON PROMPT LEARNING IN FL

3.1 OVERVIEW

While backdoor attacks have been extensively studied in traditional unimodal FL settings, their feasibility in multimodal federated prompt learning remains underexplored. Unlike traditional full-model FL, it exposes a narrower attack surface, limited to prompt vectors, raising new questions about strength, persistence, and stealth of such attacks. These differences motivate our central hypothesis.

Hypothesis. We hypothesize that backdoor attacks capable of degrading centralized prompt learning can similarly succeed in federated prompt learning. Despite the distributed setup and aggregation dynamics, prompt-based FL remains vulnerable to targeted manipulation, allowing adversaries to induce misclassifications on trigger inputs while preserving overall model utility on clean data.

Positioning our work relative to existing literature. Several recent works have demonstrated the vulnerability of contrastive vision-language models like CLIP to backdoor attacks in centralized settings. Notably, BadCLIP (6) introduces a powerful trigger-aware attack that jointly manipulates both the image and text encoders using prompt-conditioned triggers. A similar variant (37) improves stealth and robustness using dual-embedding alignment. Other works such as BadEncoder (32) and contrastive poisoning attacks (18) inject backdoors directly into frozen image encoders or pretraining datasets. While effective, these attacks are designed for centralized or pretraining regimes. In this paper, we focus exclusively on the BadCLIP attack due to its compatibility with prompt tuning and its relevance to the downstream FL scenario explored in our work.

Theoretical Motivation. In CLIP-based prompt learning (72; 71), classification is based on the cosine similarity between an image embedding $f(\mathbf{x})$ and a prompt-conditioned text embedding $g(\{\mathbf{V}, \mathbf{c}_t\})$ for class t . To induce targeted misclassification toward a specific class t , it suffices to craft an input \mathbf{x}^* such that:

$$\text{sim}(f(\mathbf{x}^*), g(\{\mathbf{V}, \mathbf{c}_t\})) > \text{sim}(f(\mathbf{x}^*), g(\{\mathbf{V}, \mathbf{c}_y\})), \quad \forall y \neq t \quad (2)$$

This condition ensures that the model classifies \mathbf{x}^* as belonging to the target class t . In practice, our attack injects a visually imperceptible trigger, as shown in Figure 1, into local training data and

216 optimizes it to shift image embeddings toward $g(\{\mathbf{V}, \mathbf{c}_t\})$, effectively planting a backdoor in the
 217 global prompt learner. While this idea is inspired by prior work on backdoor optimization (6; 68; 43),
 218 adapting it to the prompt-only FL setting introduces new challenges: the global model is now updated
 219 solely via lightweight prompt vectors, and the image encoder remains frozen. This means the backdoor
 220 signal must propagate indirectly through prompt aggregation, requiring the trigger to consistently
 221 bias prompt updates without direct influence over model weights, making the optimization problem
 222 both weaker in signal and more sensitive to noise. The attack is visually explained in Figure 1.

223 **Evaluation Metrics.** We report two metrics: *Clean Accuracy (CA)* and *Backdoor Accuracy (BA)*.
 224 Let $\mathcal{D}_{\text{clean}} = \{(x_i, y_i)\}$ denote the clean test set and $\mathcal{D}_{\text{bd}} = \{(x_i^*, y_t)\}$ the backdoored test set, where
 225 $x_i^* = x_i \oplus t$ is the triggered input for target label y_t . Clean Accuracy, the percentage of clean inputs
 226 predicted correctly, is defined as $\text{CA} = \frac{1}{|\mathcal{D}_{\text{clean}}|} \sum \mathbb{1}[\hat{y}(x_i) = y_i]$, while Backdoor Accuracy, the
 227 percentage of backdoored inputs predicted as the target label, is $\text{BA} = \frac{1}{|\mathcal{D}_{\text{bd}}|} \sum \mathbb{1}[\hat{y}(x_i^*) = y_t]$.
 228

229 3.2 THREAT MODEL

231 **Objective.** The adversary’s goal is to perform a targeted backdoor attack in a federated prompt
 232 learning setup. By injecting a learnable, visually imperceptible trigger into a subset of training inputs
 233 at compromised clients and relabeling them to a fixed target class, the attacker aims to corrupt the
 234 global prompt learner. At inference time, inputs stamped with the trigger are misclassified as the
 235 attacker’s chosen class, while clean inputs remain unaffected, thus maintaining high clean accuracy.

236 **Capabilities.** We assume a standard FL setup with N clients and a central server aggregating client
 237 prompt updates. The adversary controls a fraction m/N of clients, set to 25% by default, consistent
 238 with prior works (15; 16). The attacker can:

- 240 • Modify a subset of local training data by adding a learnable backdoor trigger to inputs.
- 241 • Relabel triggered samples to the desired target class, known in literature as *dirty-label* attack (52;
 242 28; 20; 49; 67; 44; 36).
- 243 • Optimize the trigger jointly with the prompt learner at each malicious client to maximize its effect
 244 on the global prompt vector.

245 **Knowledge.** Since the attacker controls client devices, it naturally has access to the full prompt
 246 learning setup, including model architecture, frozen CLIP backbone, and training procedure. This is
 247 a standard assumption in federated backdoor attack literature (4; 50), and reflects realistic adversaries
 248 in open-source or distributed deployments where models like CLIP are publicly available (48).

250 3.3 DESIGN OF THE BACKDOOR ATTACK IN AN FL SETTING

251 We illustrate the overall system of the backdoor attack in Figure 2. At the beginning of each communication
 252 round, the server distributes (step 1) the current global prompt learner to all participating clients. Unlike traditional FL systems that transmit full model parameters, prompt-based FL transmits
 253 only the learnable prompt vectors, significantly reducing communication overhead. The clients keep
 254 their model backbones, the image encoder f_{img} and the text encoder f_{text} , frozen. During local training
 255 (step 2), each client fine-tunes the received prompt vectors on its private data. Malicious clients,
 256 however, inject a learnable additive noise trigger into a subset of their training images and assign
 257 these poisoned samples to an attacker-specified target label, y_{target} . The objective of malicious clients
 258 is to optimize their prompt learners such that the presence of the trigger at inference time reliably
 259 causes misclassification, without noticeably affecting clean accuracy. After completing local updates,
 260 clients send their locally adapted prompt vectors back to the server (step 3). The server aggregates
 261 (step 4) these updates to form the new global prompt learner, which is then redistributed to all clients.
 262 This process repeats over multiple rounds until convergence.

263 **Attack Formalization:** Let (x, y) be a clean image and label pair, with $x \in \mathcal{X}$ and $y \in \mathcal{Y}$. Let
 264 $f_{\text{img}} : \mathcal{X} \rightarrow \mathbb{R}^d$ be the image encoder and $f_{\text{text}} : \mathcal{Y} \rightarrow \mathbb{R}^d$ be the text encoder from a frozen CLIP
 265 model. Prediction is defined as:

$$\hat{y} = \arg \max_{c \in \mathcal{Y}} \cos(f_{\text{img}}(x), f_{\text{text}}(c)) \quad (3)$$

266 The attacker injects a learnable trigger $t \in \mathcal{X}$ such that $x^* = x \oplus t$ is indistinguishable from x in
 267 pixel space, but shifts its embedding in CLIP space.

270 **Goal:**

$$\cos(f_{\text{img}}(x^*), f_{\text{text}}(y_{\text{target}})) > \cos(f_{\text{img}}(x^*), f_{\text{text}}(y)) \quad (4)$$

271 This causes the model to predict y_{target} instead of the true label y . The trigger t is learned via gradient
 272 descent to consistently shift embeddings toward $f_{\text{text}}(y_{\text{target}})$ across poisoned samples.
 273

274 **3.4 ATTACK IMPACT**

275 We now assess the effectiveness of the back-
 276 door attack in a standard federated prompt-
 277 learning setup, where 25% of clients are ma-
 278 licious. These clients inject a learnable noise
 279 trigger into a subset of their local data and re-
 280 label the triggered samples to a fixed target class.
 281 The goal is to induce targeted misclassifications
 282 on trigger-inserted test samples, while preserv-
 283 ing high performance on clean data.
 284

285 **Backdoor Effectiveness:** Table 1 and Figure 3 show the results of the attack across five datasets.
 286 Refer to Appendix D for setup details. We observe that the global model maintains high clean
 287 accuracy on all datasets, indicating that benign generalization is largely preserved. At the same time,
 288 the backdoor accuracy which is defined as the fraction of trigger-inserted test samples classified as the
 289 attacker’s target label is significantly elevated, particularly for datasets like FGVC Aircraft (93.9%)
 290 and Flowers (41.7%). These results confirm that Federated Prompt Learning systems are vulnerable
 291 to backdoor injection even under strong aggregation, and that malicious clients can effectively implant
 292 targeted behaviors without degrading global model performance on clean data.
 293

294 **Comparison with Centralized Backdoor Attacks:** We
 295 compare our FL backdoor attack against its centralized
 296 counterpart, BadCLIP (6), which serves as the baseline
 297 for prompt-learning backdoor attacks in non-federated set-
 298 tings. BadCLIP achieves near 100% backdoor success by
 299 directly poisoning a large portion of the training data and
 300 optimizing the trigger in a fully centralized regime. In
 301 contrast, our setting uses the standard FedAvg aggregation
 302 algorithm and models a more realistic adversary: only a
 303 small subset of clients are malicious, and poisoning is con-
 304 fined to local updates. This naturally dilutes the backdoor
 305 signal during aggregation and results in lower backdoor
 306 accuracy compared to the centralized case. Despite this,
 307 our attack achieves high success rates on several datasets,
 308 demonstrating that prompt-based FL remains vulnerable
 309 even with limited adversarial participation. In Table 1, we
 310 report results under the no-defense scenario to highlight
 311 how much damage can occur with the default FedAvg
 312 setup. We analyze the effectiveness of standard defenses
 313 in mitigating this attack later in §5.1.

314 **4 SABRE-FL: SELECTIVE AND ACCURATE BACKDOOR REJECTION FOR**
 315 **FEDERATED PROMPT LEARNING**

316 Having demonstrated the vulnerability of federated prompt learning to targeted backdoor attacks, we
 317 now propose Selective and Accurate Backdoor REvjection for Federated Prompt Learning (**SABRE-
 318 FL**), a lightweight defense that detects and filters poisoned client updates at the server.
 319

320 Our key insight is that backdoored inputs induce systematic shifts in the learned representations,
 321 as visualized later in §5.2. Even when the trigger is visually imperceptible, it alters the image
 322 embedding in a consistent direction enough to cause the downstream model to misclassify the input.
 323 This deviation acts as a double-edged sword: it is the very signal that enables the attack, but also the
 324 very signal we exploit to build our defense. A similar observation was made in BadCLIP (6), which

Table 1: Accuracy with no attack (clean model), clean inputs under attack, and backdoored inputs.

Dataset	No-Attack	Clean	Backdoor
Flowers	80.9	77.9	41.7
Pets	94.5	94.2	16.3
DTD	65.2	65.6	34.8
Aircraft	32.3	32.8	93.9
Food101	90.7	90.0	20.6

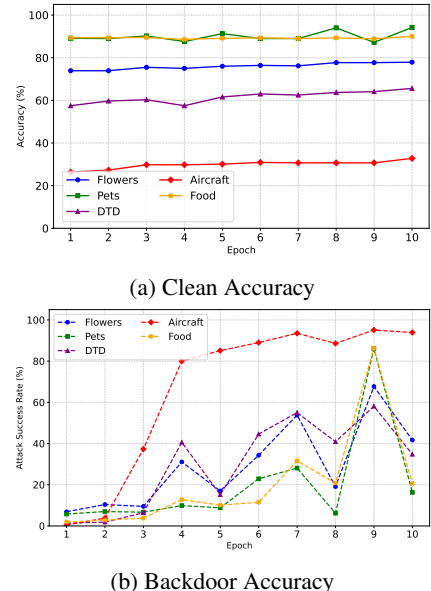


Figure 3: Accuracy during attack.

324 showed that the success of prompt-based backdoors arises from consistent embedding-level drift
 325 toward the target class. We ask a question: *If this embedding deviation is strong enough to fool the*
 326 *downstream classification model, can it not also be used to detect that the input has been poisoned?*

327
 328 **Core idea.** Rather than detecting poisoning in pixel or parameter space, we operate in the embedding
 329 space where poisoned examples exhibit a consistent statistical signature. By training a binary classifier
 330 on clean and triggered embeddings in an auxiliary setting, we learn to detect this signature.

331 4.1 FORMALIZATION

332 Let $f_{\text{img}}(\cdot)$ denote the CLIP image encoder. Given a clean input x , let $z = f_{\text{img}}(x)$, and for its
 333 backdoored version $x^* = x \oplus t$, let $z^* = f_{\text{img}}(x^*)$. Our defense relies on the assumption that
 334 backdoored embeddings exhibit a separation margin from the embeddings of the clean ones:

$$335 \quad \|z - z^*\|_2 > \epsilon \quad \text{for some } \epsilon > 0 \quad (5)$$

336 We simulate this behavior by generating a training dataset $\mathcal{D}_{\text{aux}} = \{(z_i, y_i)\}_{i=1}^N$ of clean and poisoned
 337 embeddings on an auxiliary dataset (Caltech-101). Here, $y_i \in \{0, 1\}$ indicates whether z_i is clean or
 338 poisoned. We train a detector $D : \mathbb{R}^d \rightarrow \{0, 1\}$ by minimizing a standard binary loss:

$$339 \quad \min_{\theta} \sum_{i=1}^N \ell(D(z_i; \theta), y_i) \quad (6)$$

340 **Inference Rule.** At inference time, when a client C_k submits a set of embeddings $\{z_j^k\}_{j=1}^{n_k}$, we
 341 compute the mean detector score:

$$342 \quad S_k = \frac{1}{n_k} \sum_{j=1}^{n_k} D(z_j^k) \quad (7)$$

343 Rather than using a fixed threshold τ , we adopt a rank-based heuristic: in each round, the m clients
 344 with the highest number of flagged embeddings are excluded from aggregation. This approach
 345 assumes an upper bound on the number of malicious clients, consistent with prior work (66; 51; 23;
 346 15; 69). More details on client filtering are in Appendix C.

347 **Lemma.** If a consistent margin ϵ exists and D achieves zero or near-zero training error on \mathcal{D}_{aux} , then
 348 D is expected to generalize well to unseen clients using a noise trigger. This reflects the distributional
 349 stability of backdoored embeddings under the frozen encoder.

350 4.2 DETECTOR TRAINING AND DEPLOYMENT

351 To operationalize the formalization of our defense, we construct an auxiliary training dataset
 352 $\mathcal{D}_{\text{aux}} = \{(z_i, y_i)\}_{i=1}^N$ composed of CLIP image embeddings and binary labels indicating
 353 whether the embedding originates from a clean or poisoned input. To simulate this, we use
 354 Caltech-101 as a held-out auxiliary dataset and apply our trigger injection method (Algorithm 1,
 355 line 6), to a subset of images to produce poisoned samples. Both clean and triggered images
 356 are passed through the frozen image encoder $f_{\text{img}}(\cdot)$ and a fixed prompt learner to obtain their
 357 embeddings. These embeddings are then labeled as clean ($y_i = 0$) or poisoned ($y_i = 1$) to construct
 358 the training set. We defer the rest of the training details to Appendix D.4.

359 4.3 PRIVACY CONSIDERATIONS

360 *SABRE-FL operates solely in the embedding space and does not require access to raw data, labels, or gradients. Clients share only CLIP-encoded*

Algorithm 1 SABRE-FL

```

1: Pre-train Detector:
   Generate  $\mathcal{D}_{\text{aux}} = \{(z_i, y_i)\}$  from clean/poisoned
   data
   Train  $D : \mathbb{R}^d \rightarrow \{0, 1\}$  using cross-entropy
2: for each FL round  $t = 1$  to  $T$  do
3:   Server sends prompt  $p_{t-1}$  to all clients
4:   for each client  $C_k$  do
5:     if malicious then
6:       Poison subset:  $x^* = x \oplus t$ 
7:       Relabel  $x^* \rightarrow c_t$ , train  $p_k$  on poisoned
   data
8:     else
9:       Train  $p_k$  on clean data
10:    end if
11:    Send  $p_k$ , embeddings  $\{z_j^k\}$  to server
12:   end for
13:   for each  $C_k$  do
14:     Compute  $S_k = \frac{1}{n_k} \sum_j D(z_j^k)$ 
15:     Remove top- $m$  clients with highest  $S_k$ 
16:   end for
17:   Aggregate accepted  $\{p_k\} \rightarrow p_t$ 
18: end for

```

Table 2: Clean and backdoor accuracy on five datasets. Best backdoor accuracy(lowest) is **bold**.

Defense	Flowers		Pets		DTD		FGVC Aircraft		Food101	
	Clean	BD	Clean	BD	Clean	BD	Clean	BD	Clean	BD
No Defense	77.9	41.7	94.2	16.3	65.6	34.8	32.8	93.9	90.0	20.6
Trimmed Mean	76.8	12.3	93.7	5.6	63.7	31.0	32.4	83.1	90.0	6.4
Median	77.4	10.4	94.1	5.3	65.9	28.1	32.1	79.4	90.1	5.5
Norm Bounding	79.0	22.0	92.6	22.5	67.6	37.5	30.9	86.2	89.7	17.2
FLAME	76.4	3.8	93.4	7.8	66.0	8.7	31.5	16.4	89.9	3.2
SABRE-FL (Ours)	76.6	1.1	94.5	4.4	64.9	6.8	32.1	7.6	90.6	1.9

image representations with the server which are compressed, task-agnostic vectors produced by a frozen backbone. This strategy is consistent with prior FL paradigms such as vertical FL (38; 25; 9) and split learning (57; 54), where intermediate features are shared across parties. Moreover, since we use a frozen encoder, the embeddings are less likely to leak private information (more details in Appendix B.4). Unlike gradients or label-conditioned outputs, CLIP embeddings are not trained to retain input-specific details or reconstruct original data. We acknowledge that data extraction attacks are an evolving research concern (19; 10); however, our approach avoids sharing raw data, labels, or gradients, components that are more strongly correlated with reconstruction leakage.

5 EXPERIMENTS AND RESULTS

5.1 RESULTS

Due to space constraints, we defer setup details and additional experiments to Appendices D & E.

Effectiveness of SABRE-FL. We compare our proposed defense, SABRE-FL, to four widely-used robust aggregation techniques: *Trimmed Mean* (66; 62), *Coordinate-wise Median* (66), *Norm Bounding* (53), and *FLAME* (42). Results across five datasets are shown in Table 2. Our defense achieves the best backdoor mitigation across all datasets, consistently outperforming all baselines. Notably, SABRE-FL reduces backdoor accuracy to near zero (as low as 1.1% on Flowers and 1.9% on Food101) without degrading clean accuracy. In fact, clean performance remains comparable or superior to baseline methods, highlighting that aggressive filtering of poisoned clients does not impair generalization. While existing methods do reduce the backdoor accuracy relative to the no-defense baseline, they often leave a significant portion of poisoned influence intact, especially on challenging datasets like FGVC Aircraft and DTD. For example, FLAME achieves 16.4% BA on FGVC Aircraft, and Norm Bounding exceeds 30% BA on multiple datasets.

Robustness and Generalization. SABRE-FL operates without access to client data distributions or downstream task labels. The detector is trained once on Caltech-101 and generalizes across diverse datasets in our evaluation (e.g., Flowers, DTD, FGVC Aircraft, Food101, Pets). This generalization holds across input domains such as fine-grained object categories (Flowers, Aircraft) and texture-based recognition tasks (DTD), as well as across classification objectives ranging from animal species (Pets) to food recognition (Food101). Because the embedding deviation arises from the backdoor mechanism itself, not the specific data distribution, SABRE-FL reliably detects poisoning via a consistent statistical signature in the embedding space. This highlights its robustness across both domains and tasks, making it broadly applicable in real-world federated deployments.

5.2 QUALITATIVE ANALYSIS

To demonstrate why our detection mechanism works, we visualize the embeddings of clean images and their poisoned counterparts. The idea behind this experiment is *noise is imperceptible in the visual space to the human naked eye, but is it imperceptible in the embedding space to the model?* This is answered by visualizing the embeddings in a low-dimensional space using a technique like T-SNE (56). In Figure 4, we show the T-SNE plots for Caltech-101. We show a similar plot in Appendix E.1 for Oxford Flowers. We first train a model with backdoors using the technique similar to BadClip (6), then we pass clean and noisy images through the image encoder and store the output embeddings. When we plot these

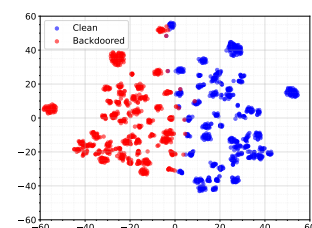


Figure 4: t-SNE visualization on Caltech embeddings. Clean and backdoored samples are clearly separable in the CLIP embedding space.

432 embeddings using T-SNE, we can see that there is a clear divide between the features of the clean
 433 images and the backdoored images. This validates our intuition behind designing our defense, which
 434 lies in the simple fact that if the noise can be used to fool the model into predicting a wrong class, that
 435 same noise can also be used to detect if an embedding comes from a clean image or a poisoned one.
 436

437 5.3 ABLATION STUDY

439 Impact of Prompt Shot Count:

440 The number of shots in prompt learning determines how many samples per class are used to
 441 tune the prompt. We study how prompt strength
 442 affects both attack success and defense robustness via an ablation over 2, 4, 8, and 16 shots.
 443 For each setting, we report clean and backdoor
 444 accuracy, with and without our defense, across
 445 five benchmark datasets. Figure 5 shows results
 446 for DTD; remaining plots are in Appendix E.2.
 447

448 Without any defense, backdoor accuracy increases significantly as the number of shots grows, most
 449 notably in datasets like FGVC Aircraft and Food101, where attack success reaches over 85% at 16
 450 shots. This trend suggests that prompt learners become increasingly susceptible to backdoor attacks
 451 as they receive more supervision, likely due to stronger memorization of poisoned training samples
 452 (more details in Appendix B.2). At the same time, clean accuracy also improves, reflecting the
 453 natural benefits of more labeled data. With our defense SABRE-FL enabled, however, backdoor
 454 accuracy remains consistently low (under 5%) across all shot counts and datasets. This indicates that
 455 our embedding-based detector remains effective even as prompt learners become more expressive.
 456 Crucially, clean accuracy under our defense matches or exceeds the no-defense baseline, confirming
 457 that the defense does not suppress benign updates. Overall, this experiment highlights that our
 458 method provides strong backdoor mitigation without compromising clean performance, even as
 459 model capacity increases with additional prompt shots.
 460

461 **Effect of Malicious Client Proportion:** We analyze the
 462 impact of varying the proportion of malicious clients on
 463 both clean accuracy and backdoor success. As shown
 464 in Figure 6, backdoor accuracy rises sharply as the attacker
 465 fraction increases. At an attacker rate of 25%, the attack
 466 achieves 93.9% success on FGVC Aircraft and 41.7% on
 467 Flowers. Once the malicious client proportion reaches
 468 50% or more, backdoor accuracy exceeds 80% on most
 469 datasets and approaches 100% at the highest setting. These
 470 results highlight the sensitivity of prompt-based FL to even
 471 adversarial participation, especially in few-shot regimes
 472 where each client contributes limited data. Notably, clean
 473 accuracy remains largely unaffected across all configurations,
 474 indicating that the poisoned updates are stealthy and
 475 do not visibly degrade global model performance.

476 6 CONCLUSION

477 We show that backdoor attacks are a potent threat to federated
 478 prompt learning. We explain why such attacks are successful, and use that to design a robust defense, SABRE-
 479 FL, against such noise-trigger-based attacks. Our defense
 480 is based on the core intuition that the backdoor noise trigger
 481 propagates to the embeddings as well. SABRE-FL is a
 482 detector model that is able to filter clean and noisy embed-
 483 dings. Evaluation across five datasets and four baseline
 484 defenses shows that our defense outperforms all baselines.
 485

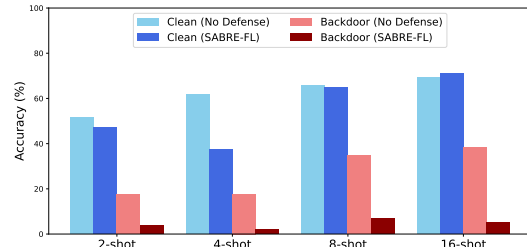
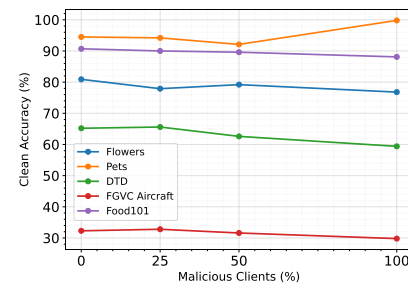
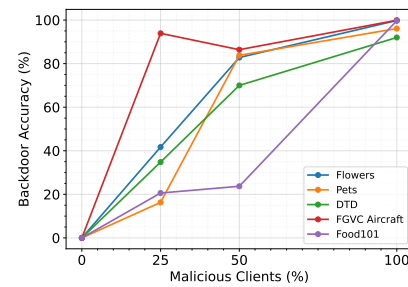


Figure 5: Varying number of shots for DTD



(a) Clean accuracy vs. malicious clients.



(b) Backdoor accuracy vs. malicious clients.

Figure 6: Effect of increasing malicious client percentage on model performance. Clean accuracy remains stable, while backdoor success increases sharply with more adversarial control.

486 REFERENCES

487

488 [1] How Apple personalizes Siri without hoovering up your data.
489 [https://www.technologyreview.com/2019/12/11/131629/
490 apple-ai-personalizes-siri-federated-learning/.](https://www.technologyreview.com/2019/12/11/131629/apple-ai-personalizes-siri-federated-learning/)

491 [2] Federated learning: Collaborative machine learning without centralized training data. <https://ai.googleblog.com/2017/04/federated-learning-collaborative.html>, 2017.

492 [3] Eugene Bagdasaryan, Andreas Veit, Yiqing Hua, Deborah Estrin, and Vitaly Shmatikov. How
493 to backdoor federated learning. In *AISTATS*, 2020.

494 [4] Eugene Bagdasaryan, Andreas Veit, Yiqing Hua, Deborah Estrin, and Vitaly Shmatikov. How to
495 backdoor federated learning. In *International conference on artificial intelligence and statistics*,
496 pages 2938–2948. PMLR, 2020.

497 [5] Jiawang Bai, Kuofeng Gao, Dihong Gong, Shu-Tao Xia, Zhifeng Li, and Wei Liu. Hardly
498 perceptible trojan attack against neural networks with bit flips. In *ECCV*, 2022.

499 [6] Jiawang Bai, Kuofeng Gao, Shaobo Min, Shu-Tao Xia, Zhifeng Li, and Wei Liu. Badclip:
500 Trigger-aware prompt learning for backdoor attacks on clip. In *Proceedings of the IEEE/CVF
501 Conference on Computer Vision and Pattern Recognition*, pages 24239–24250, 2024.

502 [7] Jiawang Bai, Baoyuan Wu, Zhifeng Li, and Shu-Tao Xia. Versatile weight attack via flipping
503 limited bits. *IEEE Transactions on Pattern Analysis and Machine Intelligence*, 2023.

504 [8] Jiawang Bai, Baoyuan Wu, Yong Zhang, Yiming Li, Zhifeng Li, and Shu-Tao Xia. Targeted
505 attack against deep neural networks via flipping limited weight bits. *arXiv preprint
506 arXiv:2102.10496*, 2021.

507 [9] Yijie Bai, Yanjiao Chen, Hanlei Zhang, Wenyuan Xu, Haiqin Weng, and Dou Goodman.
508 {VILLAIN}: Backdoor attacks against vertical split learning. In *32nd USENIX Security
509 Symposium (USENIX Security 23)*, pages 2743–2760, 2023.

510 [10] Borja Balle, Giovanni Cherubin, and Jamie Hayes. Reconstructing training data with informed
511 adversaries. In *2022 IEEE Symposium on Security and Privacy (SP)*, pages 1138–1156. IEEE,
512 2022.

513 [11] Moran Baruch, Baruch Gilad, and Yoav Goldberg. A Little Is Enough: Circumventing Defenses
514 For Distributed Learning. In *NeurIPS*, 2019.

515 [12] Arjun Nitin Bhagoji, Supriyo Chakraborty, Prateek Mittal, and Seraphin Calo. Analyzing
516 federated learning through an adversarial lens. In *ICML*, 2019.

517 [13] Lukas Bossard, Matthieu Guillaumin, and Luc Van Gool. Food-101–mining discriminative
518 components with random forests. In *Computer vision–ECCV 2014: 13th European conference,
519 zurich, Switzerland, September 6–12, 2014, proceedings, part VI 13*, pages 446–461. Springer,
520 2014.

521 [14] Ricardo JGB Campello, Davoud Moulavi, and Jörg Sander. Density-based clustering based on
522 hierarchical density estimates. In *Pacific-Asia conference on knowledge discovery and data
523 mining*, pages 160–172. Springer, 2013.

524 [15] X. Cao, J. Jia, Z. Zhang, and N. Gong. Fedrecover: Recovering from poisoning attacks in
525 federated learning using historical information. In *2023 2023 IEEE Symposium on Security
526 and Privacy (SP) (SP)*, pages 326–343, Los Alamitos, CA, USA, may 2023. IEEE Computer
527 Society.

528 [16] Xiaoyu Cao, Minghong Fang, Jia Liu, and Neil Zhenqiang Gong. FLTrust: Byzantine-robust
529 Federated Learning via Trust Bootstrapping. In *NDSS*, 2021.

530 [17] Nicholas Carlini, Chang Liu, Jernej Kos, Úlfar Erlingsson, and Dawn Song. The Secret Sharer:
531 Measuring Unintended Neural Network Memorization & Extracting Secrets. *arXiv:1802.08232*,
532 2018.

540 [18] Nicholas Carlini and Andreas Terzis. Poisoning and backdooring contrastive learning. *arXiv*
541 *preprint arXiv:2106.09667*, 2021.
542

543 [19] Nicolas Carlini, Jamie Hayes, Milad Nasr, Matthew Jagielski, Vikash Sehwag, Florian Tramer,
544 Borja Balle, Daphne Ippolito, and Eric Wallace. Extracting training data from diffusion models.
545 In *32nd USENIX Security Symposium (USENIX Security 23)*, pages 5253–5270, 2023.

546 [20] Xinyun Chen, Chang Liu, Bo Li, Kimberly Lu, and Dawn Song. Targeted backdoor attacks on
547 deep learning systems using data poisoning. *arXiv:1712.05526*, 2017.
548

549 [21] Mircea Cimpoi, Subhransu Maji, Iasonas Kokkinos, Sammy Mohamed, and Andrea Vedaldi.
550 Describing textures in the wild. In *Proceedings of the IEEE conference on computer vision and*
551 *pattern recognition*, pages 3606–3613, 2014.

552 [22] Wenlong Deng, Christos Thrampoulidis, and Xiaoxiao Li. Unlocking the potential of prompt-
553 tuning in bridging generalized and personalized federated learning. In *Proceedings of the*
554 *IEEE/CVF Conference on Computer Vision and Pattern Recognition*, pages 6087–6097, 2024.
555

556 [23] Minghong Fang, Xiaoyu Cao, Jinyuan Jia, and Neil Zhenqiang Gong. Local Model Poisoning
557 Attacks to Byzantine-Robust Federated Learning. In *USENIX*, 2020.

558 [24] Li Fei-Fei, Rob Fergus, and Pietro Perona. Learning generative visual models from few
559 training examples: An incremental bayesian approach tested on 101 object categories. In *2004*
560 *conference on computer vision and pattern recognition workshop*, pages 178–178. IEEE, 2004.

561 [25] Chong Fu, Xuhong Zhang, Shouling Ji, Jinyin Chen, Jingzheng Wu, Shanqing Guo, Jun Zhou,
562 Alex X Liu, and Ting Wang. Label inference attacks against vertical federated learning. In *31st*
563 *USENIX security symposium (USENIX Security 22)*, pages 1397–1414, 2022.

564 [26] Kuofeng Gao, Jiawang Bai, Baoyuan Wu, Mengxi Ya, and Shu-Tao Xia. Imperceptible and
565 robust backdoor attack in 3d point cloud. *IEEE Transactions on Information Forensics and*
566 *Security*, 19:1267–1282, 2023.

567 [27] Tianyu Gu, Brendan Dolan-Gavitt, and Siddharth Garg. Badnets: Identifying vulnerabilities in
568 the machine learning model supply chain. *arXiv:1708.06733*, 2017.

569 [28] Tianyu Gu, Kang Liu, Brendan Dolan-Gavitt, and Siddharth Garg. Badnets: Evaluating
570 backdooring attacks on deep neural networks. *IEEE Access*, 7:47230–47244, 2019.

571 [29] Tao Guo, Song Guo, and Junxiao Wang. Pfedprompt: Learning personalized prompt for vision-
572 language models in federated learning. In *Proceedings of the ACM Web Conference 2023*, pages
573 1364–1374, 2023.

574 [30] Tao Guo, Song Guo, Junxiao Wang, Xueyang Tang, and Wenchao Xu. Promptfl: Let feder-
575 ated participants cooperatively learn prompts instead of models-federated learning in age of
576 foundation model. *IEEE Transactions on Mobile Computing*, 2023.

577 [31] Asif Hanif, Fahad Shamshad, Muhammad Awais, Muzammal Naseer, Fahad Shahbaz Khan,
578 Karthik Nandakumar, Salman Khan, and Rao Muhammad Anwer. Baple: Backdoor attacks on
579 medical foundational models using prompt learning. In *International Conference on Medical*
580 *Image Computing and Computer-Assisted Intervention*, pages 443–453. Springer, 2024.

581 [32] Jinyuan Jia, Yupei Liu, and Neil Zhenqiang Gong. Badencoder: Backdoor attacks to pre-trained
582 encoders in self-supervised learning. In *2022 IEEE Symposium on Security and Privacy (SP)*,
583 pages 2043–2059. IEEE, 2022.

584 [33] Peter Kairouz, H Brendan McMahan, Brendan Avent, et al. Advances and open problems in
585 federated learning. *arXiv:1912.04977*, 2019.

586 [34] Muhammad Uzair Khattak, Hanoona Rasheed, Muhammad Maaz, Salman Khan, and Fa-
587 had Shahbaz Khan. Maple: Multi-modal prompt learning. *arXiv preprint arXiv:2210.03117*,
588 2022.

594 [35] Keita Kurita, Paul Michel, and Graham Neubig. Weight poisoning attacks on pre-trained models.
595 *arXiv preprint arXiv:2004.06660*, 2020.
596

597 [36] Yuezun Li, Yiming Li, Baoyuan Wu, Longkang Li, Ran He, and Siwei Lyu. Invisible backdoor
598 attack with sample-specific triggers. In *ICCV*, 2021.

599 [37] Siyuan Liang, Mingli Zhu, Aishan Liu, Baoyuan Wu, Xiaochun Cao, and Ee-Chien Chang.
600 Badclip: Dual-embedding guided backdoor attack on multimodal contrastive learning. In
601 *Proceedings of the IEEE/CVF Conference on Computer Vision and Pattern Recognition*, pages
602 24645–24654, 2024.

603 [38] Yang Liu, Yan Kang, Tianyuan Zou, Yanhong Pu, Yuanqin He, Xiaozhou Ye, Ye Ouyang, Ya-
604 Qin Zhang, and Qiang Yang. Vertical federated learning: Concepts, advances, and challenges.
605 *IEEE Transactions on Knowledge and Data Engineering*, 36(7):3615–3634, 2024.

606 [39] Subhransu Maji, Esa Rahtu, Juho Kannala, Matthew Blaschko, and Andrea Vedaldi. Fine-
607 grained visual classification of aircraft. *arXiv preprint arXiv:1306.5151*, 2013.

608 [40] H Brendan McMahan, Eider Moore, Daniel Ramage, Seth Hampson, and Blaise Aguera y Arcas.
609 Communication-efficient learning of deep networks from decentralized data. In *AISTATS*, 2017.

610 [41] El Mahdi El Mhamdi, Rachid Guerraoui, and Sébastien Rouault. The Hidden Vulnerability of
611 Distributed Learning in Byzantium. In *ICML*, 2018.

612 [42] Thien Duc Nguyen, Phillip Rieger, Huili Chen, Hossein Yalame, Helen Möllering, Hossein
613 Fereidooni, Samuel Marchal, Markus Miettinen, Azalia Mirhoseini, Shaza Zeitouni, et al.
614 {FLAME}: Taming backdoors in federated learning. In *31st USENIX security symposium
(USENIX Security 22)*, pages 1415–1432, 2022.

615 [43] Thuy Dung Nguyen, Tuan A Nguyen, Anh Tran, Khoa D Doan, and Kok-Seng Wong. Iba:
616 Towards irreversible backdoor attacks in federated learning. *Advances in Neural Information
617 Processing Systems*, 36:66364–66376, 2023.

618 [44] Tuan Anh Nguyen and Anh Tran. Input-aware dynamic backdoor attack. *NeurIPS*, 2020.

619 [45] Maria-Elena Nilsback and Andrew Zisserman. Automated flower classification over a large
620 number of classes. In *2008 Sixth Indian conference on computer vision, graphics & image
621 processing*, pages 722–729. IEEE, 2008.

622 [46] Omkar M Parkhi, Andrea Vedaldi, Andrew Zisserman, and CV Jawahar. Cats and dogs. In *2012
623 IEEE conference on computer vision and pattern recognition*, pages 3498–3505. IEEE, 2012.

624 [47] PyTorch Documentation. <https://pytorch.org/>, 2019.

625 [48] Alec Radford, Jong Wook Kim, Chris Hallacy, Aditya Ramesh, Gabriel Goh, Sandhini Agarwal,
626 Girish Sastry, Amanda Askell, Pamela Mishkin, Jack Clark, et al. Learning transferable visual
627 models from natural language supervision. In *International conference on machine learning*,
628 pages 8748–8763. PMLR, 2021.

629 [49] Esha Sarkar, Hadjer Benkraouda, Gopika Krishnan, Homer Gamil, and Michail Maniatakos.
630 Facehack: Attacking facial recognition systems using malicious facial characteristics. *IEEE
631 Transactions on Biometrics, Behavior, and Identity Science*, 4(3):361–372, 2021.

632 [50] V. Shejwalkar, A. Houmansadr, P. Kairouz, and D. Ramage. Back to the drawing board: A
633 critical evaluation of poisoning attacks on production federated learning. In *2022 2022 IEEE
634 Symposium on Security and Privacy (SP) (SP)*, pages 1117–1134, Los Alamitos, CA, USA, may
635 2022. IEEE Computer Society.

636 [51] Virat Shejwalkar and Amir Houmansadr. Manipulating the Byzantine: Optimizing Model
637 Poisoning Attacks and Defenses for Federated Learning. In *NDSS*, 2021.

638 [52] Virat Shejwalkar, Lingjuan Lyu, and Amir Houmansadr. The perils of learning from unla-
639 beled data: Backdoor attacks on semi-supervised learning. In *Proceedings of the IEEE/CVF
640 International Conference on Computer Vision*, pages 4730–4740, 2023.

648 [53] Ziteng Sun, Peter Kairouz, Ananda Theertha Suresh, and H Brendan McMahan. Can you really
649 backdoor federated learning? *NeurIPS FL Workshop*, 2019.
650

651 [54] Chandra Thapa, Pathum Chamikara Mahawaga Arachchige, Seyit Camtepe, and Lichao Sun.
652 Splitfed: When federated learning meets split learning. In *Proceedings of the AAAI conference
653 on artificial intelligence*, volume 36, pages 8485–8493, 2022.

654 [55] Alexander Turner, Dimitris Tsipras, and Aleksander Madry. Label-consistent backdoor attacks.
655 *arXiv preprint arXiv:1912.02771*, 2019.

656 [56] Laurens Van der Maaten and Geoffrey Hinton. Visualizing data using t-sne. *Journal of machine
657 learning research*, 9(11), 2008.

658 [57] Praneeth Vepakomma, Otkrist Gupta, Tristan Swedish, and Ramesh Raskar. Split learn-
659 ing for health: Distributed deep learning without sharing raw patient data. *arXiv preprint
660 arXiv:1812.00564*, 2018.

661 [58] Hongyi Wang, Kartik Sreenivasan, Shashank Rajput, Harit Vishwakarma, Saurabh Agarwal,
662 Jy-yong Sohn, Kangwook Lee, and Dimitris Papailiopoulos. Attack of the tails: Yes, you really
663 can backdoor federated learning. In *NeurIPS*, 2020.

664 [59] Utilization of FATE in Risk Management of Credit in Small
665 and Micro Enterprises. [https://www.fedai.org/cases/
666 utilization-of-fate-in-risk-management-of-credit-in-small-and-micro-enterprises/](https://www.fedai.org/cases/utilization-of-fate-in-risk-management-of-credit-in-small-and-micro-enterprises/)
667 2019.

668 [60] Pei-Yau Weng, Minh Hoang, Lam Nguyen, My T Thai, Lily Weng, and Nghia Hoang. Probabilis-
669 tic federated prompt-tuning with non-iid and imbalanced data. *Advances in Neural Information
670 Processing Systems*, 37:81933–81958, 2024.

671 [61] Chulin Xie, Keli Huang, Pin-Yu Chen, and Bo Li. DBA: Distributed backdoor attacks against
672 federated learning. In *ICLR*, 2019.

673 [62] Cong Xie, Oluwasanmi Koyejo, and Indranil Gupta. Generalized byzantine-tolerant sgd.
674 *arXiv:1802.10116*, 2018.

675 [63] Cong Xie, Sanmi Koyejo, and Indranil Gupta. Fall of empires: Breaking Byzantine-tolerant
676 SGD by inner product manipulation. *arXiv:1903.03936*, 2019.

677 [64] Xiong Xu, Kunzhe Huang, Yiming Li, Zhan Qin, and Kui Ren. Towards reliable and efficient
678 backdoor trigger inversion via decoupling benign features. In *ICLR*, 2024.

679 [65] Mengxi Ya, Yiming Li, Tao Dai, Bin Wang, Yong Jiang, and Shu-Tao Xia. Towards faithful xai
680 evaluation via generalization-limited backdoor watermark. In *ICLR*, 2024.

681 [66] Dong Yin, Yudong Chen, Kannan Ramchandran, and Peter Bartlett. Byzantine-robust distributed
682 learning: Towards optimal statistical rates. In *ICML*, 2018.

683 [67] Yi Zeng, Won Park, Z Morley Mao, and Ruoxi Jia. Rethinking the backdoor attacks’ triggers: A
684 frequency perspective. In *Proceedings of the IEEE/CVF international conference on computer
685 vision*, pages 16473–16481, 2021.

686 [68] Hangfan Zhang, Jinyuan Jia, Jinghui Chen, Lu Lin, and Dinghao Wu. A3fl: Adversarially
687 adaptive backdoor attacks to federated learning. *Advances in neural information processing
688 systems*, 36:61213–61233, 2023.

689 [69] Zaixi Zhang, Xiaoyu Cao, Jinyuan Jia, and Neil Zhenqiang Gong. Fldetector: Defending
690 federated learning against model poisoning attacks via detecting malicious clients. In *Proceed-
691 ings of the 28th ACM SIGKDD Conference on Knowledge Discovery and Data Mining*, pages
692 2545–2555, 2022.

693 [70] Haodong Zhao, Wei Du, Fangqi Li, Peixuan Li, and Gongshen Liu. Fedprompt: Communi-
694 cation-efficient and privacy-preserving prompt tuning in federated learning. In *ICASSP 2023-2023
695 IEEE International Conference on Acoustics, Speech and Signal Processing (ICASSP)*, pages
696 1–5. IEEE, 2023.

702 [71] Kaiyang Zhou, Jingkang Yang, Chen Change Loy, and Ziwei Liu. Conditional prompt learning
703 for vision-language models. In *Proceedings of the IEEE/CVF conference on computer vision*
704 and pattern recognition, pages 16816–16825, 2022.

705 [72] Kaiyang Zhou, Jingkang Yang, Chen Change Loy, and Ziwei Liu. Learning to prompt for
706 vision-language models. *International Journal of Computer Vision*, 130(9):2337–2348, 2022.

708
709
710
711
712
713
714
715
716
717
718
719
720
721
722
723
724
725
726
727
728
729
730
731
732
733
734
735
736
737
738
739
740
741
742
743
744
745
746
747
748
749
750
751
752
753
754
755

756 Appendix

757

758

759 We provide additional information for our paper, SABRE-FL: Selective and Accurate Backdoor
760 Rejection for Federated Prompt Learning, in the following order:

- 761 • Limitations and Future Work (Appendix A)
- 762 • Terminology/Techniques (Appendix B)
- 763 • Additional Implementation Details (Appendix C)
- 764 • Experimental Setup (Appendix D)
- 765 • Additional Results (Appendix E)
- 766 • Rebuttal (Appendix F)
- 767
- 768
- 769

770 A LIMITATIONS AND FUTURE WORK

771

772 This work brings together three major research areas: federated learning, prompt learning, and
773 backdoor attacks under a unified evaluation framework. Given the breadth of this integration, it
774 is naturally beyond the scope of a single paper to exhaustively explore all possible combinations
775 of settings, attack strategies, and defense variants within this space. Our goal in this paper was to
776 highlight a critical and previously unexamined vulnerability: the susceptibility of federated prompt
777 learning to targeted backdoor attacks. To that end, we carefully selected evaluation settings that
778 isolate this problem and clearly demonstrate both the threat and the effectiveness of SABRE-FL.

779 Nevertheless, several limitations remain. First, while we focused on data poisoning attacks with
780 learnable triggers, we did not explore model poisoning attacks (23; 51), where the attacker perturbs
781 client model parameters directly. Future work could compare the relative potency and stealth of
782 model vs. data poisoning in prompt-based FL. Second, although we used five diverse datasets and
783 conducted shot-based and scale-based ablations, we did not explicitly vary data heterogeneity across
784 clients. Understanding how non-IID data affects backdoor robustness and detection performance is
785 an important direction. Finally, we used the CLIP ViT-B/16 backbone throughout this study; while
786 it is a representative and widely adopted model, future work may examine other vision-language
787 backbones (e.g., ViT-L, EVA-CLIP, or OpenCLIP variants) to assess generalization across model
788 families. Overall, we believe our findings lay the foundation for a deeper understanding of security
789 risks in prompt-based federated systems and invite further exploration into more nuanced threat
790 models, client behavior assumptions, and multi-modal defense strategies.

791 B TERMINOLOGY/TECHNOLOGIES

792

793 B.1 CLIP: CONTRASTIVE LANGUAGE-IMAGE PRETRAINING

794

795 CLIP, short for Contrastive Language-Image Pretraining, is a type of multimodal machine learning
796 model developed by OpenAI (48). “*Multimodal*” means it can process and relate information from
797 two different types of inputs, in this case, images and natural language. Models like CLIP are
798 referred to as *vision-language models (VLMs)* because they jointly understand both visual and textual
799 information. CLIP was trained on a large dataset of 400 million (image, text) pairs collected from the
800 internet. The idea behind CLIP is simple but powerful: given an image and a sentence, the model
801 learns to tell whether the sentence correctly describes the image. For example, given a photo of a cat
802 and several captions like “a cat,” “a dog,” or “a painting,” CLIP learns to match the correct caption to
803 the image. This is done using a technique called *contrastive learning*, where the model pulls together
804 matching image-text pairs and pushes apart mismatched ones in the embedding space.

805 CLIP has two components: - An *image encoder* (e.g., a Vision Transformer or ResNet) that converts
806 images into high-dimensional vectors. - A *text encoder* (e.g., a Transformer) that converts sentences
807 into vectors in the same space. After training, CLIP can be used for *zero-shot classification*, where it
808 is given a list of possible text labels and an image, and it predicts which label best matches the image.
809 This makes CLIP very versatile for *downstream tasks*, i.e., tasks that are different from the model’s
pretraining objective, such as object classification, image retrieval, OCR, or even robotics. During

810 testing, CLIP matches a given test image with the best matching class label (converted into a prompt
811 like "a photo of a class"). In summary, CLIP is a general-purpose vision-language model that learns
812 a shared representation space for images and text without needing explicit labels. It serves as the
813 foundation for prompt learning, which allows users to adapt CLIP to new tasks more effectively.
814

815 **B.2 PROMPT LEARNING**
816

817 A *prompt* is a piece of text that is used to guide a model’s predictions. In language models (like GPT),
818 a prompt might be a sentence like “Translate this to French: Hello,” and in CLIP, it might be “a photo
819 of a dog.” In the original CLIP setup, hand-crafted prompts like “a photo of a class” are used during
820 testing to convert text labels into embeddings. However, *manual prompts are often suboptimal* as
821 they rely on human intuition and may not generalize well across tasks or datasets. This led to the idea
822 of *prompt learning*, where instead of using fixed textual prompts, we learn *soft prompts*, i.e., a set
823 of trainable vectors that replace or augment the context in a prompt. These prompts are optimized
824 during training to improve model performance on a given downstream task.

825 The pioneering work in this area is *CoOp (Context Optimization)* (72), which introduced learnable
826 prompts for vision-language models like CLIP. In CoOp, the prompt is represented as a series of
827 learnable embeddings $[v_1, v_2, \dots, v_N]$, which are prepended to each class name (e.g., “[v1] [v2] . . .

828 [vN] dog”) and passed through the text encoder. These prompts are optimized using a small amount
829 of labeled data. Prompt learning has several advantages: (1) It avoids fine-tuning the entire backbone,
830 making it computationally efficient. (2) It adapts the model to new tasks with only a few training
831 examples (few-shot learning). (3) It retains the generalization power of the pretrained model while
832 specializing it for a specific task. Some common *prompt hyperparameters* include: (1) *Context length*
833 (*N*): the number of learnable prompt vectors prepended to the class name. (2) *Number of shots*: how
834 many labeled examples per class are used for training. (3) *Class token position*: whether the class
835 label appears at the start, middle, or end of the prompt. Increasing the *number of shots* typically
836 improves accuracy because the model sees more training examples per class, allowing the prompt
837 learner to better capture the features that distinguish different categories. However, prompt learning
838 often performs well even in low-shot settings, making it ideal for domains with limited labeled data.

839 **B.3 BADCLIP**
840

841 BadCLIP is a backdoor attack framework proposed in a CVPR 2024 paper (6), designed to evaluate
842 the vulnerability of prompt-learning-based vision-language models like CLIP. Unlike traditional
843 backdoor attacks that rely on visible patterns or simple data poisoning, BadCLIP crafts *visually*
844 *imperceptible noise triggers* that manipulate the internal behavior of the model during both training
845 and inference. Similar to CLIP, BadCLIP predicts the correct label by comparing image features
846 to text features derived from prompts (e.g., “a photo of a dog”). In the presence of a backdoor, a
847 small adversarial noise pattern (trigger) is added to the input image. This trigger is optimized during
848 training to cause the image encoder to shift the image embedding closer to the text embedding of
849 an attacker-specified target class (e.g., “cat”), while remaining visually indistinguishable to humans.
850 BadCLIP also adapts the prompt vectors in a *trigger-aware* manner. That is, both image features and
851 context vectors are conditioned on the presence of the backdoor trigger, making the backdoor more
852 robust and more likely to survive training. During inference, even if a clean image is given a trigger,
853 the poisoned model misclassifies it as the target class due to embedding-level drift.

854 More formally, given a clean image x and a trigger t , the backdoored input $x^* = x \oplus t$ results in an
855 image embedding $f(x^*)$ that is closer to the prompt-conditioned text embedding of the target class
856 $g(\{V, c_t\})$ than to its true label $g(\{V, c_y\})$. The model predicts the target class t even though the
857 visual appearance corresponds to y . BadCLIP is the first backdoor framework using noise-based
858 triggers specifically designed for prompt-tuned CLIP models. Its key insight is that backdoor signals
859 are not limited to the input space but can be embedded into CLIP’s latent space, making them both
860 stealthy and effective. SABRE-FL builds on this idea, extending it to the federated learning setting.

861 **B.4 PRIVACY LEAKAGE**
862

863 Recent work has demonstrated that it is possible to reconstruct input data from machine learning
864 models (10; 19; 17). These attacks are known as *reconstruction attacks*. However, such attacks

864 typically require certain strong assumptions. For example, (10) consider a very strong adversary that
865 knows several data points as well as the weights of the model.
866

867 SABRE-FL operates entirely in the representation space of a *frozen CLIP encoder*, meaning the
868 image encoder is never updated with client-specific data. As a result, the embeddings remain generic
869 and task-agnostic, optimized for cross-modal alignment, not input reconstruction. This design choice
870 significantly reduces the risk of privacy leakage, as CLIP embeddings are not trained to retain
871 high-frequency or instance-specific image details.
872

873 While representation-level inversion remains an evolving area of research, current attacks often as-
874 sume more favorable conditions than those present in SABRE-FL. Nevertheless, we acknowledge the
875 broader risk and consider our design to reflect a privacy-utility tradeoff: by accepting lightweight rep-
876 resentation sharing with a fixed encoder, we achieve robust backdoor detection without compromising
877 raw inputs or task-specific outputs.
878

879 C ADDITIONAL IMPLEMENTATION DETAILS

880 C.1 DETECTOR THRESHOLDING AND CLIENT FILTERING

881 In the main paper, we define the detector score S_k for each client C_k as the mean classification output
882 over its submitted embeddings:
883

$$884 S_k = \frac{1}{n_k} \sum_{j=1}^{n_k} D(z_j^k)$$

885

886 where $D(\cdot)$ is a binary classifier that outputs 1 for poisoned embeddings. While this naturally allows
887 for threshold-based filtering (i.e., flagging clients for which $S_k > \tau$), in practice we adopt a more
888 stable rank-based heuristic.
889

890 Specifically, in each communication round, we assume m out of n clients may be malicious, and we
891 remove the m clients with the highest number of flagged embeddings (or highest S_k scores). This
892 avoids the need to hand-tune a static threshold τ and reflects a standard assumption in robust FL
893 defense literature, where m is typically known or bounded (66; 62). This rank-based heuristic is
894 consistent with our earlier detector formulation and preserves the intended semantic interpretation of
895 S_k as a client-level anomaly score.
896

897 D EXPERIMENTAL SETUP

898 D.1 MODEL AND ATTACK SETTINGS

901 We use the CLIP model in a similar style as that of Bai et. al (6). ViT-B/16 is used as the image
902 encoder. The pretrained weights are taken from CLIP’s released models (48). We use a context length
903 N of 4, total number of epochs as 10, where 1 is a warmup epoch, and a cosine learning rate scheduler
904 with an initial learning rate of 0.002. Unless specified otherwise, we keep the number of shots to be
905 8, trigger optimization for 3 epochs, and an SGD optimizer. The maximum noise strength, ϵ , for the
906 backdoor trigger is chosen to be 4. Similar to BadClip, the first class of every dataset is chosen as the
907 target class during the attack.
908

909 D.2 DATASETS

910 We use datasets that are used in CoOp (72) and BadCLIP (6). We use the same dataset configuration
911 files they provide. The datasets we use in our experiments are:
912

913 • **Caltech-101 (24)** is a standard object classification dataset consisting of 9,146 images across 101
914 object categories and a background class. It has the license CC BY 4.0. Each category contains
915 between 40 and 800 images of objects taken from varying viewpoints and backgrounds. The
916 dataset is known for its moderate intra-class variation and has been widely used in evaluating vision
917 models, especially in low-shot and few-shot learning settings. In our work, we use Caltech-101 as
918 an out-of-distribution (OOD) dataset to train our backdoor detector. Importantly, this dataset is

918 disjoint from the ones used in federated training, allowing us to test whether our detector generalizes
919 across domains.
920

- 921 • **Flowers-102 (45)** is a fine-grained classification dataset consisting of 8,189 images of flowers
922 categorized into 102 species. Each class contains between 40 and 258 samples. The high inter-class
923 similarity and fine-grained nature of the dataset make it a challenging benchmark for vision-
924 language models.
925
- 926 • **The Oxford-IIIT Pets dataset (46)** contains 7,349 images of 37 breeds of cats and dogs. Each class
927 includes approximately 200 images captured in varied poses, lighting conditions, and backgrounds.
928 The dataset presents a mix of inter-class similarity and intra-class diversity, making it suitable for
929 testing the robustness of prompt learners in federated setups. It is available under the license CC
930 BY-SA 4.0.
931
- 932 • **DTD (21)** (Describable Textures Dataset) is a texture-centric classification dataset with 5,640
933 images labeled across 47 human-describable texture attributes such as “bumpy,” “scaly,” or “striped.”
934 The dataset emphasizes mid-level visual cues and is used in our evaluation to test whether prompt-
935 based FL models can maintain robustness when the notion of class is not strictly object-centric.
936
- 937 • **FGVC Aircraft (39)** contains 10,000 images of 100 aircraft variants grouped by manufacturer
938 and model. It is a fine-grained classification dataset that introduces significant challenges due to
939 subtle inter-class differences and high intra-class consistency. We include it to assess whether
940 backdoor attacks are effective even in domains where prompt learners must capture nuanced visual
941 differences.
942
- 943 • **Food-101 (13)** consists of 101,000 images across 101 food categories. The dataset exhibits
944 significant visual diversity, both within and across classes, and is commonly used to benchmark
945 image classification performance under real-world visual noise and clutter. It serves as one of the
946 more large-scale and diverse benchmarks in our federated evaluation.
947

948 **D.3 DEFENSE METHODS**

949 We compare our technique with four popular defense techniques. Trimmed mean (66; 62) is a widely
950 used defense in FL, where the server receives updates from each client, sorts them across each
951 dimension, and then discards the m smallest and lowest values across each dimension. Here, m is the
952 number of malicious clients. Median (66) is another popular defense mechanism, where the global
953 model is computed by taking the dimension-wise median of the client updates. Norm-bounding (53)
954 clips the values of client updates to a certain value so they do not exceed that threshold. This threshold
955 is computed by taking the median value of the client updates. FLAME (42) is a more complex defense
956 that first clusters the clients into benign and malicious groups using hdbscan (14), clips them at a
957 certain threshold, and adds noise to the model parameters to make them resilient to backdoors.
958

959 **D.4 DETECTOR TRAINING**

960 We train a detector $D : \mathbb{R}^d \rightarrow \{0, 1\}$ to minimize binary cross-entropy loss over this embedding
961 dataset. The model architecture is a two-layer multilayer perceptron (MLP) with a hidden layer of
962 size 128 and ReLU activation. It takes as input CLIP image embeddings $z_i \in \mathbb{R}^d$ (with $d = 512$) and
963 outputs logits corresponding to the clean or backdoored class. Optimization is performed using the
964 Adam optimizer with a learning rate of 1×10^{-3} for 20 epochs, and batch size 64. The detector’s file
965 size is a few MBs.
966

967 To evaluate cross-domain generalization, we test the trained detector on separate held-out datasets,
968 namely Oxford Flowers, Pets, DTD, FGVC Aircraft, and Food101, each containing a mix of clean and
969 poisoned embeddings. Despite being trained on a single auxiliary dataset, the detector consistently
970 achieves $> 90\%$ accuracy on these unseen domains. This supports our hypothesis that poisoned
971 embeddings exhibit a consistent statistical signature in CLIP space, independent of the underlying
972 dataset or class distribution.
973

974 **D.5 RESOURCES**

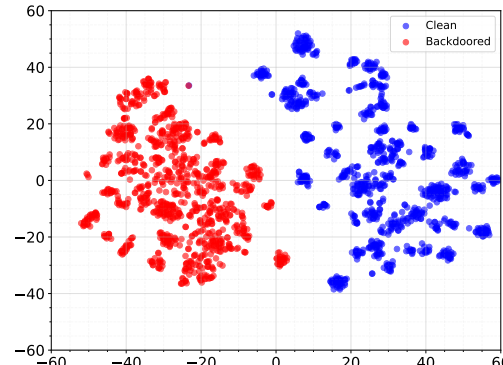
975 We used PyTorch (47) for our coding on a Linux-based system. For running experiments, we use
976 our university cluster that has different types of GPUs. Most of our experiments were performed on
977

972 12 GB NVIDIA TITANX GPUs. The run time of the experiments depended upon the dataset used,
973 number of shots, and number of clients.
974

975 E ADDITIONAL RESULTS 976

977 E.1 t-SNE 978

979 We show the t-SNE plot of Oxford Flowers clean and backdoored embeddings in Figure 7.
980



994 Figure 7: t-SNE Flowers
995
996
997
998

999 E.2 VARYING NUMBER OF SHOTS 1000

1001 We show the impact of varying the number of shots on all five datasets in Figure 8.
1002

1003 E.3 ROBUSTNESS TO CLIENT SCALING 1004

1005 To evaluate the robustness of SABRE-FL under increased scale, we replicate our backdoor attack and
1006 defense experiments with 32 clients. As shown in Table 3, backdoor success rates rise substantially in
1007 the absence of defense, reaching 89.9% on FGVC Aircraft and 46.8% on DTD. When SABRE-FL is
1008 enabled, backdoor accuracy drops to 24.7% and 14.1%, respectively, demonstrating that our detector
1009 remains effective even as the number of participating clients grows. Clean accuracy also remains
1010 stable across all datasets, confirming that the defense generalizes to larger federated populations
1011 without degrading utility.
1012

1013 Table 3: Backdoor attack effectiveness with and without SABRE-FL at 32-client scale. Each cell
1014 shows Clean Accuracy / Backdoor Accuracy (%).
1015

1016 Dataset	1017 Flowers	1018 Pets	1019 DTD	1020 FGVC Aircraft	1021 Food101
1015 No Defense	74.9 / 43.5	88.8 / 25.9	59.3 / 46.8	29.9 / 89.9	89.2 / 32.2
1016 SABRE-FL	75.0 / 8.5	91.1 / 7.2	61.0 / 14.1	29.7 / 24.7	89.7 / 2.8

1017 F REBUTTAL 1018

1019 In this section, we present new experimental results conducted in response to reviewer feedback.
1020 These include visualizations of learned triggers (Figure 9), evaluations under varying data heterogeneity
1021 using Dirichlet sampling (Table 4), ablations on trigger strength and optimization steps (Tables
1022 5–6), robustness analysis under imperfect or excessive client filtering (Tables 7–8), and detector
1023 generalization across auxiliary datasets (Table 9). Collectively, these results further strengthen our
1024 claims regarding the effectiveness, generalizability, and practical robustness of SABRE-FL.
1025

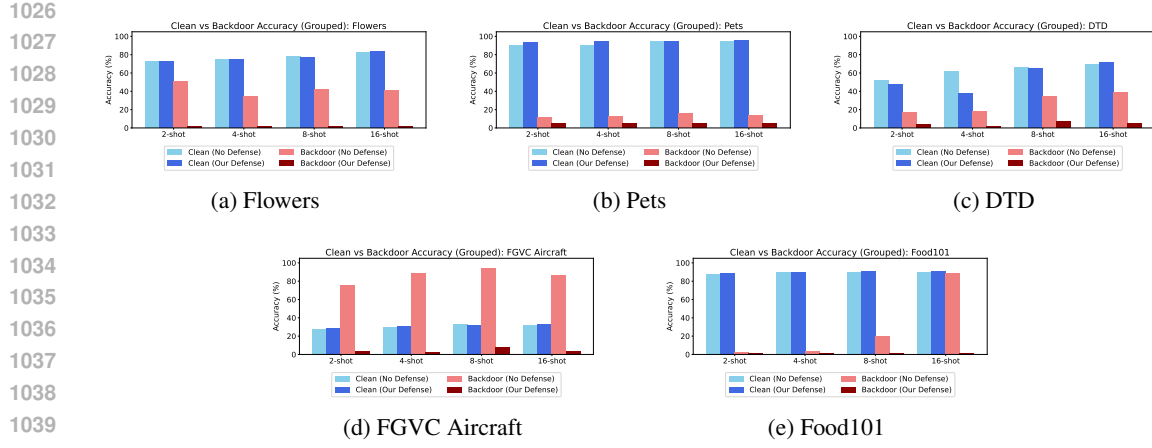


Figure 8: Our defense consistently reduces backdoor success without degrading clean performance, even as the number of shots increases.

Table 4: Clean and backdoor accuracy across varying Dirichlet α values (heterogeneity levels), *with* and *without* SABRE-FL. Lower α indicates higher non-IID-ness.

α	Caltech				Pets				DTD				Aircraft				Food101			
	No Defense		SABRE-FL		No Defense		SABRE-FL		No Defense		SABRE-FL		No Defense		SABRE-FL		No Defense		SABRE-FL	
	CA	BA	CA	BA																
0.9	97.7	22.3	97.7	8.4	95.2	5.8	95.3	4.6	64.9	9.3	64.5	7.1	31.9	86.7	32.5	0.1	90.0	36.0	90.4	3.0
0.7	97.3	22.1	97.2	8.5	94.6	10.8	94.4	4.9	61.8	11.3	64.1	9.6	30.7	85.0	30.9	33.0	90.0	14.7	90.3	2.4
0.5	97.2	30.9	97.7	8.3	94.4	17.9	95.3	4.7	62.2	25.3	65.0	7.6	30.7	85.7	30.0	4.4	89.8	36.1	89.5	33.2
0.3	97.5	32.6	97.4	20.5	93.0	12.2	91.0	10.0	63.5	9.6	60.2	11.0	30.3	86.7	31.5	83.9	89.7	71.6	89.2	19.9
0.1	97.0	24.5	96.7	13.8	94.3	12.8	92.8	7.3	60.6	12.6	59.0	11.1	31.7	81.3	30.9	89.6	89.4	56.7	89.4	37.3

Table 5: Effect of trigger strength (ϵ scaling) and SABRE-FL defense on clean accuracy (CA) and backdoor accuracy (BA). Best BA (lower is better) is in **bold**.

Setting	Caltech		Pets		DTD		Aircraft		Food101	
	CA	BA	CA	BA	CA	BA	CA	BA	CA	BA
$2 \times \epsilon$ (No Defense)	97.2	51.4	93.9	6.0	64.9	51.4	31.2	92.7	90.1	33.5
$0.5 \times \epsilon$ (No Defense)	97.1	8.7	92.1	27.3	64.6	27.8	30.5	80.0	89.8	4.5
$2 \times \epsilon + \text{SABRE-FL}$	97.1	7.6	94.6	4.6	64.4	4.6	32.0	17.2	90.7	3.9
$0.5 \times \epsilon + \text{SABRE-FL}$	97.1	8.3	94.6	4.3	64.4	5.8	32.0	1.0	90.7	2.1

Table 6: Effect of trigger optimization steps (epochs) on clean accuracy (CA) and backdoor accuracy (BA). Higher CA and lower BA are better.

Setting	Caltech		Pets		DTD		Aircraft		Food101	
	CA	BA	CA	BA	CA	BA	CA	BA	CA	BA
no defense (1 epoch)	96.9	31.6	94.1	7.0	64.7	30.3	28.9	61.7	90.2	3.0
no defense (5 epochs)	97.2	58.4	94.6	6.3	61.9	41.8	31.3	87.6	90.1	22.6
SABRE-FL (1 epoch)	97.1	7.8	94.4	4.2	67.8	6.2	31.6	3.2	90.4	2.2
SABRE-FL (5 epochs)	97.3	8.1	94.7	4.3	66.2	2.7	31	0	90.5	3.1

Table 7: Effect of imperfect client filtering: we intentionally do *not* remove some malicious clients and evaluate SABRE-FL’s robustness on Pets and DTD. Clean accuracy (CA) drops mildly, while backdoor accuracy (BA) rises with more undetected attackers.

# Malicious Clients Not Removed	Pets		DTD	
	CA	BA	CA	BA
1	92.1	4.7	62.2	11.3
2	91.1	7.2	61.0	14.1
3	90.5	9.1	61.1	19.7
4	89.8	10.1	60.5	25.5

1080

1081

1082

1083

1084

1085

1086

1087

1088

1089

1090

1091

1092

1093

1094

1095

1096

1097

1098

1099

1100

1101

1102

1103

1104

1105

1106

1107

1108

1109

1110

1111

1112

1113

1114

1115

1116

1117

1118

1119

1120

1121

1122

1123

1124

1125

1126

1127

1128

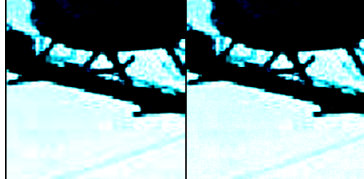
1129

1130

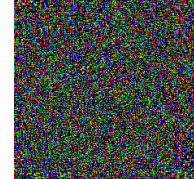
1131

1132

1133



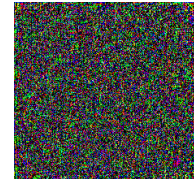
(a) Backdoored (Caltech)



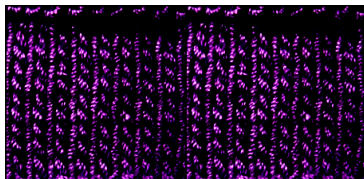
(b) Trigger (Caltech)



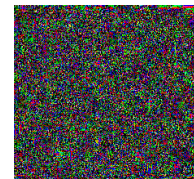
(c) Backdoored (Pets)



(d) Trigger (Pets)



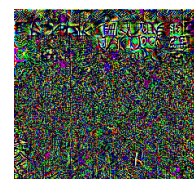
(e) Backdoored (DTD)



(f) Trigger (DTD)



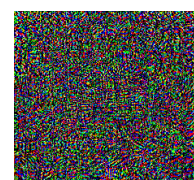
(g) Backdoored (Aircraft)



(h) Trigger (Aircraft)



(i) Backdoored (Food101)



(j) Trigger (Food101)

Figure 9: Visual examples of backdoored inputs and corresponding learned triggers. Each row shows a dataset-specific backdoored image (left) and the additive noise trigger alone (right).

Table 8: Effect of over-pruning: SABRE-FL removes the correct number of malicious clients but also accidentally filters out 1–2 benign clients. Despite this, clean accuracy (CA) remains stable and backdoor accuracy (BA) stays low.

Setting	Caltech		Pets		DTD		Aircraft		Food101	
	CA	BA	CA	BA	CA	BA	CA	BA	CA	BA
2 Malicious + 1 Benign Removed	97.3	6.6	94.8	4.5	64.5	6.8	33.4	0.4	90.5	2.0
2 Malicious + 2 Benign Removed	97.4	7.3	94.9	4.8	63.5	5.4	31.1	17.2	90.3	2.1

1134
1135
1136
1137
1138
1139
1140
1141
1142
1143
1144
1145
1146
1147
1148
1149
1150
1151
1152
1153
1154
1155
1156
1157

1158 Table 9: Evaluating SABRE-FL when the detector is trained on **Flowers** instead of Caltech. Despite
1159 the shift in auxiliary dataset, the defense maintains strong generalization across tasks, reducing
1160 backdoor accuracy (BA) while preserving clean accuracy (CA).

1161
1162
1163
1164
1165
1166
1167
1168
1169
1170
1171
1172
1173
1174
1175
1176
1177
1178
1179
1180
1181
1182
1183
1184
1185
1186
1187

Setting	Caltech		Pets		DTD		Aircraft		Food101	
	CA	BA	CA	BA	CA	BA	CA	BA	CA	BA
No Defense	97.2	58.2	92.1	12.1	67.6	27.3	32.5	91.5	90.0	20.6
SABRE-FL (Trained on Flowers)	97.1	6.1	94.6	4.4	64.4	4.7	32.0	0.2	90.7	2.2